euronoise

Aeroacoustic Computation of Ducted-Fan Broadband Noise Using LES Data

Gabriel Reboul, Cyril Polacsek, Serge Lewy and Sebastien Heib

ONERA, 29 avenue Division Leclerc, 92320 Châtillon, France
gabriel.reboul@onera.fr

Following large efforts to reduce tone noise during the last decades in modern high bypass ratio turbofans, fan broadband noise reduction has become an industrial priority. Improvement of broadband noise prediction tools are required and have motivated the present study. A hybrid computational method providing source to far-field prediction of turbofan broadband noise is presented. The proposed acoustic model is based on the loading noise term of the Ffowcs Williams and Hawkings (FW-H) equation with a modal Green's function, and on a Kirchhoff approximation for the free-field radiation. The aerodynamic sources on the airfoils required by the model are issued from a Large Eddy Simulation (LES) computation. The first part of the study is concerned with the LES data. Usual assumptions about coherence and energy distribution between the acoustic modes are analyzed. Then, first predictions are compared to available measurements in the DLR low speed fan laboratory rig. Finally, far-field predictions using Kirchhoff integral are compared to exact solutions using a Wiener-Hopf technique.

1 Introduction

Aircraft noise reduction is now a major priority for manufacturers since air traffic is growing and environmental rules are becoming drastic. With the increase of bypass ratio of modern turbofans, fan broadband noise contribution is almost the same as the tones in terms of overall level. This motivates the development of accurate methods able to simulate this contribution.

The aeroacoustic problem can be split in three parts: sources generation, in-duct propagation, and far-field radiation. Several complex turbulence mechanisms involved in turbofan broadband noise have been identified, but it is admitted that interactions between rotor wakes and stator vanes are dominant. In-duct acoustic field is obtained from the FW-H equation, generalized by Goldstein [1] to ducted problems by introducing an expanded modal form of the Green's function. Analytical turbulent spectra and blade response models have generally been adopted [2], but recent improvements in LES computations are making possible direct calculations by integrating the LES turbulent pressure disturbances along vanes surfaces, as is done in this paper. Although exact solutions based on the Wiener-Hopf technique are available for semi-infinite circular and annular ducts [3, 4], acoustic radiation from inlet or exhaust is simply achieved here by means of a Kirchhoff integral. It is clearly shown in the paper that the Kirchhoff approximation is quite reliable. A sketch of the present methodology is illustrated on Fig.1.

The hybrid method is applied to a simplified rotor-stator interaction relative to a low speed fan [5, 6]. Stator surface pressures computed by LES are analyzed, and in-duct sound pressure and power spectra predicted by the acoustic model are compared to the measurements. Finally, despite the fact that no experimental data is available, free-field radiation is also discussed by comparing Wiener-Hopf and Kirchhoff solutions.

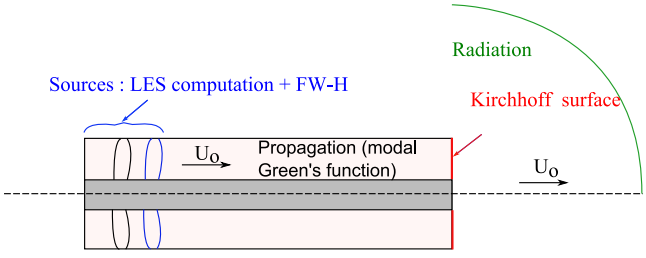

Figure 1: Fan broadband noise prediction scheme

2 LES computation of a rotor-stator interaction

2.1 Configuration and numerical grid

Computations are made on the DLR low speed fan configuration [5]. The ducted fan consists in a 24-bladed rotor and $V = 16$ outlet guide vanes (OGV) with 87.7 mm in span length. The geometry at the source location is annular, the tip radius is equal to 226.5 mm, and the hub-to-tip ratio is 0.613. Downstream, the duct becomes cylindrical and the radius, R, grows up to 250 mm. The results presented in this paper correspond to the baseline configuration, i.e. an inlet Mach number $M = 0.04$, a pressure ratio of 1.014, and a rotor speed of 3220 rpm (blade tip Mach number of 0.22).

The LES computation is performed using the ONERA code *elsA*, considering a few restrictions. The numerical grid should extend along an azimuth of $\pi/4$ to include three blade channels and two vane channels. However, only one blade channel is kept to minimize the grid size, connected to one vane channel. This would not be valid for the tones because it would change the propagating interaction modes. It seems to be acceptable for broadband noise since only the aerodynamic field between blades can be slightly modified. Also, span length of the stator is reduced to 4.32 mm which is equal to the boundary layer thickness at the trailing edge of the OGV. It is also of the same order as the measured radial turbulence length scale. The LES structured grid around a rotor blade and a stator vane is made of several blocks (Fig.2) with a total of 6,307,501 nodes in the rotor frame and 5,881,113 in the stator frame.

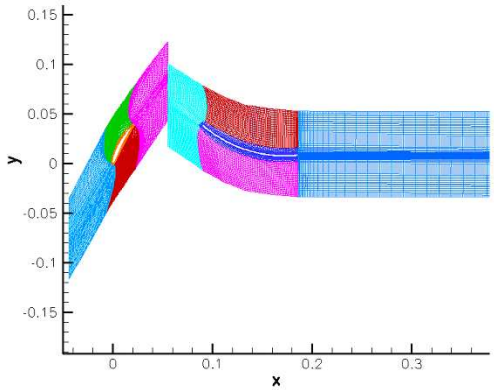

Figure 2: Multiblock LES grid (axis in meters)

Tip radius geometrical characteristics of the fan are used in the computation (Table 1). The blade-to-blade spacing is 88.83 mm, and the spacing from blade trailing edge (TE) to OGV leading edge (LE) is 69 mm.

Rotor		Stator	
Chord	43.5 mm	Chord length	104 mm
Max thickness	3.6 mm	Thickness	2 mm
Stagger angle	27.4 deg	LE angle	36.9 deg
		TE angle	-6.3 deg

Table 1: Geometrical characteristics of the fan at the tip radius

2.2 Stator surface pressure analysis

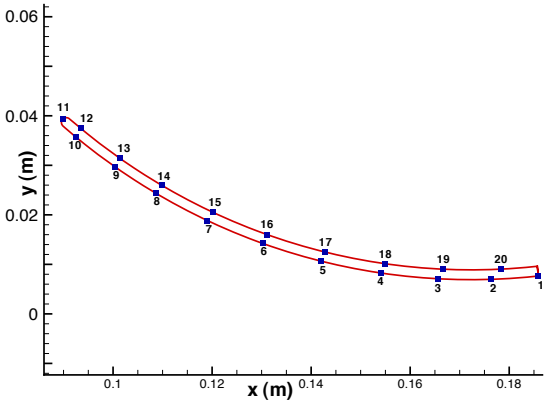

Figure 3: Input data locations on the vane

Fig.3 shows the 20 selected points as input data. The time step is equal to $\Delta t = 1.3\ \mu s$ (one every ten points of the LES iterations), and the total simulation duration available for the present calculations is $T = 16.4$ ms. Some time signatures are shown in Fig.4.

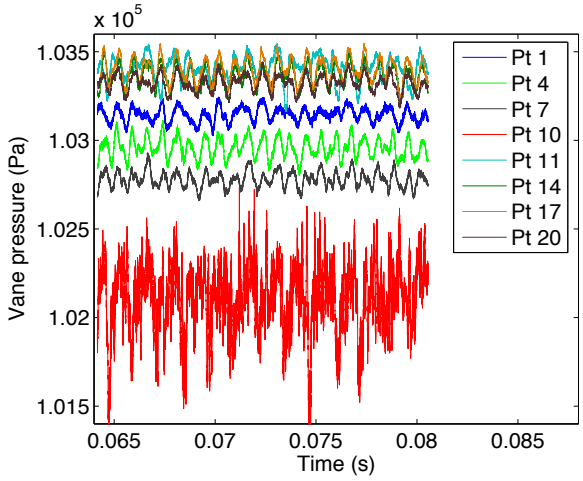

Figure 4: Vane pressure time signatures

Signatures appear to be highly correlated one to each others. Lower level and higher fluctuations relative to point 10 are probably due to a flow detachment, whereas the flow seems to reattach downstream. Because the signature duration is rather short, the power spectral density (PSD) is computed with a large frequency step, $\Delta f = 366$ Hz, in order to make some averages (8 averages with a small overlapping are used here).

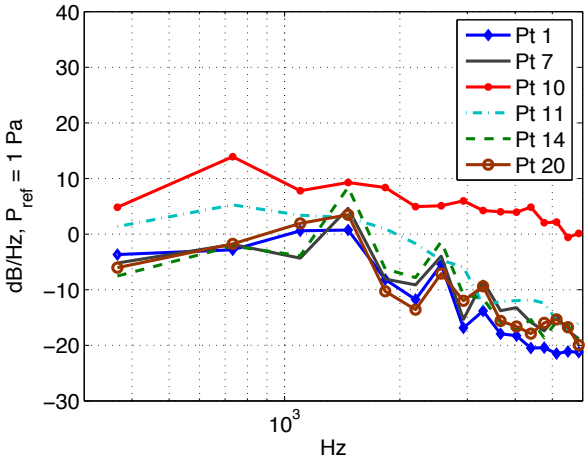

Figure 5: Vane pressure power spectral densities

The blade passage frequency (BPF) is equal to 800 Hz, but emerging tones at 1500 and 2500 Hz are still unexplained. Such peaks could be attributed to acoustic resonances (standing waves) due to numerical reflections at the inlet and outlet boundaries of the stator frame grid. Higher pressure fluctuations at points 10 and 11 for which BPF tone is dominant and can be due to the fact that these points are less affected by the reflections. Improved computations are underway in order to solve this problem.

3 Acoustic computation

3.1 Ducted-fan broadband noise propagation

The acoustic propagation model assumes the main following hypotheses: (i) Hard walled duct, (ii) Semi-infinite duct (no reflection at the duct exit), (iii) Constant cross section (annular or cylindrical) and (iv) Uniform axial flow. Sources and observers positions are defined in cylindrical coordinates as:

$$Observer(\overrightarrow{X}) : \left\| \begin{matrix} r \\ \theta \\ z \\ t \end{matrix} \right. \quad Source(\overrightarrow{Y}) : \left\| \begin{matrix} r_s \\ \theta_s \\ z_s \\ \tau \end{matrix} \right. \qquad (1)$$

Acoustic pressure

The starting point is the well known FW-H equation limited to the dipole term:

$$p\left(\overrightarrow{X},t\right) = \int_{-T}^{T}\int_{S_Y} F_i(\overrightarrow{Y},\tau)\frac{\partial G}{\partial y_i}dS_Y d\tau \qquad (2)$$

where $p\left(\overrightarrow{X},t\right)$ is the acoustic pressure fluctuation, F is the unsteady load on the vane surface and G is the Green's function. The formulation follows Ventres [7] and Lewy [8]. Pressure modal expansion, with $A_{m\mu}$ the modal amplitude, is:

$$\hat{p}\left(\overrightarrow{X},f\right)=\sum_{m\mu}\hat{p}_{m\mu}\left(\overrightarrow{X},f\right) \quad (3)$$

$$\hat{p}_{m\mu}\left(\overrightarrow{X},f\right)=\sum_{m\mu}A_{m\mu}C_{m\mu}(\alpha_{m\mu}\frac{r_s}{R})e^{-i(m\theta+k_{m\mu}z)} \quad (4)$$

where $k_{m\mu}$ is the axial wavenumber, $\alpha_{m\mu}$ is the duct eigenvalue for mode $(m\mu)$. As the LES computation is made on a single strip of span length Δr, sources are duplicated in the spanwise direction. Strips are considered incoherent since Δr is of the same order as the integral length scale. So the modal amplitude for one vane on a strip j is given by:

$$A^j_{m\mu}(f)=\frac{1}{2\Gamma}\int_{l_s}\left[k_{m\mu}n_z+\frac{m}{r_s(j)}n_\theta\right]\frac{\hat{P}\left(\overrightarrow{Y},f\right)}{\Delta_{m\mu}}$$
$$\times C_{m\mu}(\alpha_{m\mu}\frac{r_s(j)}{R})e^{i(m\theta_s+k_{m\mu}z_s)}\Delta r dl_s \quad (5)$$

n_z and n_θ are respectively the axial and circumferential components of the unit vector normal to the airfoil surface. This unit vector and the curvilinear spacing dl_s along the profile are deduced from the vane surface LES mesh. Rienstra's normalization [9] is used to express the duct eigenfunction, $C_{m\mu}$, so that the normalizing factor Γ is equal to $2\pi R^2$. $\Delta_{m\mu}$ is related to the dispersion relationship and $\hat{P}\left(\overrightarrow{Y},f\right)$ is the Fourier transform of the vane pressure.

Acoustic power

The well known acoustic power expression, valid for an isentropic fluid with a uniform axial velocity is used:

$$W_{m\mu}\|_{duct}=\frac{\Gamma}{2\rho_0 c_0}\frac{k(\beta^2 k_{m\mu}+Mk)}{(k-Mk_{m\mu})^2}|A_{m\mu}(f)|^2 \quad (6)$$

where $\beta=\sqrt{1-M^2}$ is the Lorentz's factor.

Power spectral density

The PSD for the stationary random pressure signal is related to Eq (4) as:

$$S_{pp}(f)=\lim_{T\to+\infty}\frac{V}{2T}\sum_j E\left[\sum_{m\mu}\hat{p}^j_{m\mu}(f)^*\sum_{m'\mu'}\hat{p}^j_{m'\mu'}(f)\right] \quad (7)$$

E is the ensemble average and vanes are supposed uncorrelated. Modal summations are made over all propagating modes.
If modes are considered uncorrelated the PSD becomes:

$$S_{pp}(f)=\lim_{T\to+\infty}\frac{V}{2T}\sum_j\sum_{m\mu}E\left[\left|\hat{p}^j_{m\mu}(f)\right|^2\right] \quad (8)$$

Hence, the PSD for the acoustic power is obtained as:

$$S_{ww}(f)=\lim_{T\to+\infty}\frac{V}{2T}\sum_j\sum_{m\mu}\frac{\Gamma}{2\rho_0 c_0}$$
$$\times\frac{k(\beta^2 k_{m\mu}+Mk)}{(k-Mk_{m\mu})^2}E\left[\left|A^j_{m\mu}(f)\right|^2\right] \quad (9)$$

As turbulent mechanisms generate random dipole distributions along the rows, acoustic propagating modes are very often assumed to be uncorrelated when estimating the Sound Pressure Level (SPL). It is proposed here to check the validity of this assumption by computing the SPL using Eq (7) or (8).

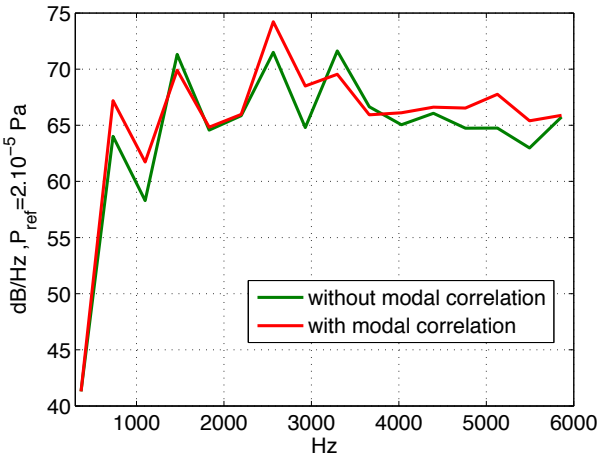

Figure 6: SPL with and without modal correlation

Fig.6 shows the SPL at 1 meter from the sources, at the duct wall. The same analysis is made (Fig.7) with the Overall Sound Pressure Level (OASPL) in an axial duct section. Even if differences can be important at some frequencies and locations, when looking at broadband component, the fact that numerous modes are propagating tend to cancel the cross-term of Eq (7). This point can be advantageous with respect to CPU time requirement, or when coupling with advanced propagation models (i.e. Euler equations) involving CAA (which will be also investigated at ONERA in a further step).

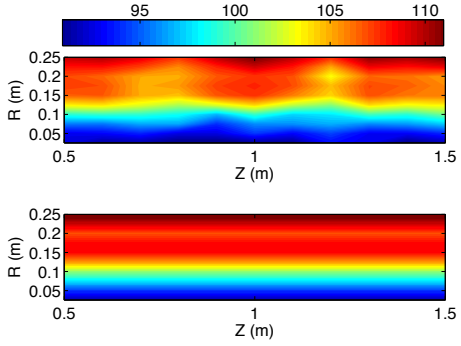

Figure 7: OASPL [0 - 6KHz] with (top) and without (bottom) modal correlation

3.2 Comparisons between prediction and measurements

The method presented in the previous section is applied to the DLR configuration. As the annular part is rather short compared to the cylindrical part, a cylindrical geometry is considered in the calculations to better fit the acoustic power distribution at microphone locations. Behaviour of annular and cylindrical geometries with respect to cut-on modes has been found almost

negligible. The axial mean Mach number is set equal to 0.04. Experimental data have been provided by DLR, using method described in [5] for the sound Power Level (PWL) determination. We can note that tones have been removed in the PWL data. Only downstream computation results are presented here. The SPL data are averaged over 4 microphones (see [5]) using the non-coherent mode assumption. Calculation-measurement comparison are presented in Figs.8 and 9.

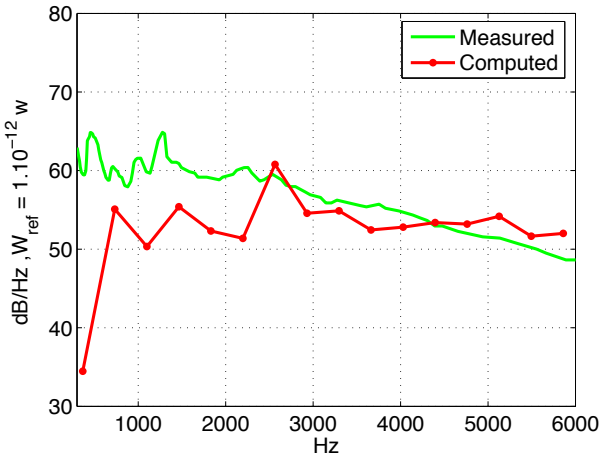

Figure 8: In-duct (downstream) PWL prediction

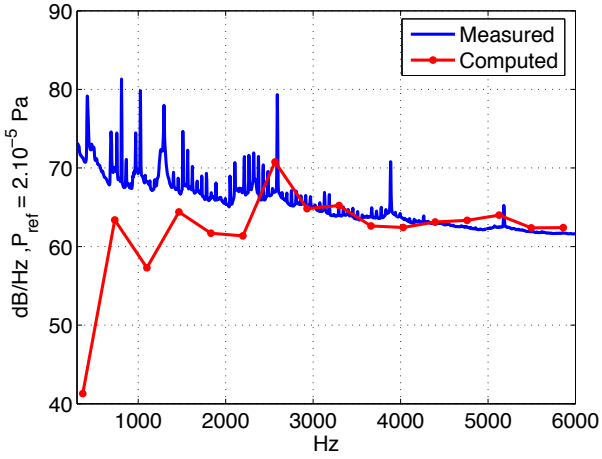

Figure 9: In-duct (downstream) SPL prediction

Beyond the low frequency range (0-2500 Hz), PWL and SPL predictions are in a good agreement with the measurements. Since numerous sources are not predicted with LES (secondary flow, interaction with boundary layer, etc.), a reasonable explanation could be that these sources are predominant at low frequency as observed in [6]. Furthermore, the strong correlations emphasized by the surface pressure analyzes lead to an over-estimation of the levels characterized by the emerging peaks at 800, 1500 and 2500 Hz.

3.3 Free-field radiation

An objective of this section is a comparison between a simple and fast way to compute far-field radiation using a Kirchhoff approximation and an exact solution more complicated and CPU time consuming, involving a Wiener-Hopf technique.

Formulations

The Kirchhoff formulation, extending the Tyler and Sofrin model, can be applied in a uniform axial flow and computation can be done above 90° since the duct exit has not to be flanged. The formulation is detailed in [8]. For comparison with Kirchhoff, the exact formulation used hereafter follows Homicz and Lordi [4] for a cylindrical duct in uniform motion. In both formulations, the radiated pressure without mean flow at the observer position M (D, θ, φ, in spherical coordinates), with a far-field approximation ($kD \gg 1$) can be expressed as:

$$p_r\left(\overrightarrow{M},t\right) = A_{m\mu} D_{m\mu} \frac{e^{i(\omega t - kD - k_{m\mu} Z_{Sv} - m\theta)}}{D} \qquad (10)$$

Z_{sv} is the distance between sources and duct exit plane along the z-axis. $D_{m\mu}$ is the directivity factor which varies from a formulation to another. For the broadband computation, modes are taken uncorrelated. Thus, the acoustic power in free-field for low Mach number is obtained as:

$$W_{m\mu}(f)\,\|_{free} = \frac{\pi D^2}{\rho_0 c_0} \int_0^{\pi} (1 + M cos(\varphi))^2 \times \left|\hat{p_r}\left(\overrightarrow{M},f\right)\right|^2 sin(\varphi) d\varphi \qquad (11)$$

Results

For the application, the same Mach number as before is used, computation is made at $D = 10R$, in order to satisfy to the far-field approximation. OASPL is given in Fig.10. Very good agreement is found until 90° but as

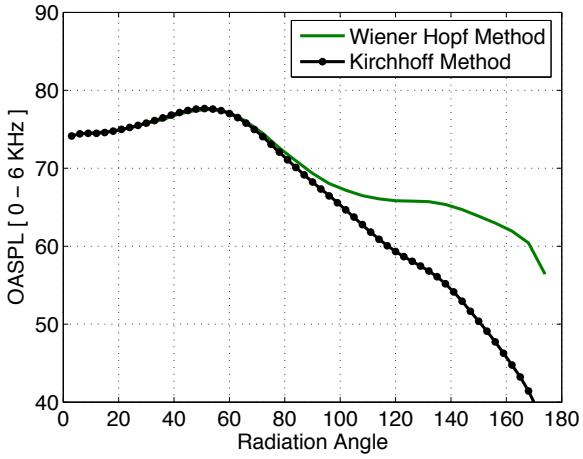

Figure 10: OASPL at 2.5 m from the exhaust

expected, levels above 90° are badly predicted using the Kirchhoff method. Except at very low frequencies, the power computation in Fig.11 shows that levels above 90° are low enough not to influence the spectrum. Energy conservation is well assessed. Principal sources of error when using Kirchhoff are listed below. Firstly, the integration surface here is limited to the duct exit section,

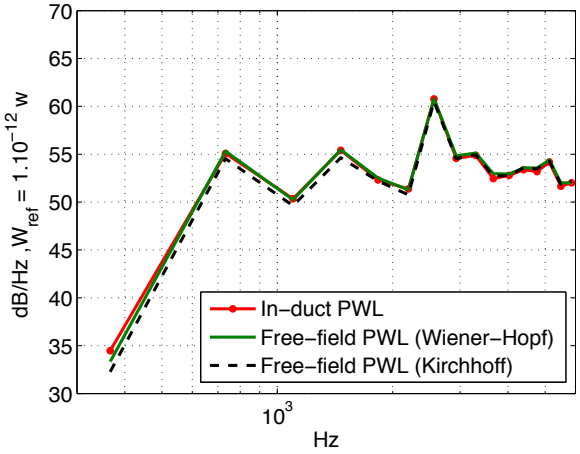

Figure 11: In-duct and free-field power level

whereas it should normally surround all the sources. Secondly, the Kirchhoff integral does not take into account reflection at the exit, since the sources on the surface are determined for an infinite duct and modes near cut off might be over-estimated. That is why it is interesting to compare contributions of modes near and far cut-off frequency. Fig.12 exhibits contribution

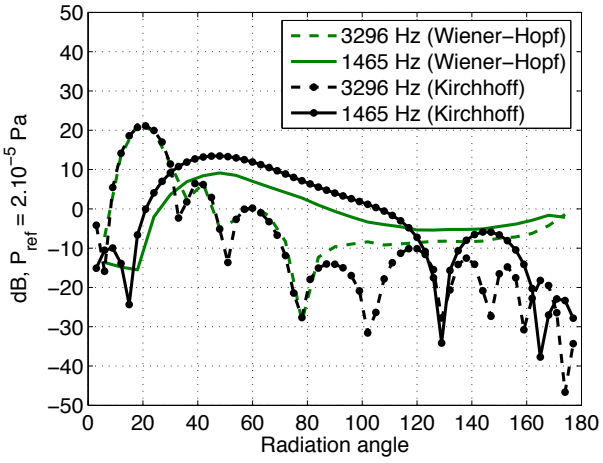

Figure 12: SPL of mode (1,2) near (1465 Hz) and far (3296 Hz) cut off

of mode (1,2) at 1465 Hz and 3296 Hz. The cut-off frequency of this mode is 1145 Hz. Results confirm the over-estimation for modes near cut off using Kirchhoff. But, Fig.11 shows that the effect of this over-estimation is not important because modes near cut off are not numerous and their contribution is weaker.

4 Conclusions and future developments

A hybrid method devoted to source-to-far-field prediction of broadband noise generated by rotor-stator interactions in turbofan engines has been developed and applied to a simplified configuration. An integral formulation based on the FW-H equation has been coupled to a LES computation providing the turbulent-source inputs. First comparisons with experimental data in terms of shape and level of in-duct PSD are rather good. However, a few problems in the LES data have to be solved (unexpected tones and high correlation). The uncorrelated mode assumption usually adopted has been checked as well as the use of Kirchhoff approximation to calculate the far-field radiation (by comparing the results with the Wiener-Hopf solutions). Future improvements will concern the LES data reliability, and also the possibility to use additional informations (from experiments or RANS computations) in order to better model the 3D (spanwise) effects in the computation chain.

Acknowledgments

This study has been carried out within the EU-funded project PROBAND.

References

[1] M.E. Goldstein. *Aeroacoustics*. McGraw-Hill International Book Company, New york, (1976).

[2] B. de Gouville, M. Roger, and J.M. Cailleau. "Prediction of fan broadband noise". In *AIAA Paper 98-2317*, (1998).

[3] G. Gabard and R.J. Astley. "Theoretical model for sound radiation from annular jet pipe: far- and near-field solutions". *Journal of Fluid Mechanics*, 549:315–341, (2006).

[4] G.F. Homicz and J.A. Lordi. "A note on the radiative directivity patterns of duct acoustic modes". *Journal of Sound and Vibration*, 41 (3):283–290, (1975).

[5] L. Enghardt, L. Neuhaus, and C. Lowis. "Broadband sound power determination in flow ducts". In *AIAA Paper 2004-2940*, (2004).

[6] V. Jurdic, A. Moreau, P. Joseph, L. Engardt, and J. Coupland. "A comparaison between measured and predicted fan broadband noise due to rotor-stator interaction". In *AIAA Paper 2007-3692*, (2007).

[7] C.S. Ventres, M.A. Theobald, and W.D. Mark. "Turbofan noise generation , Volume 1 : Analysis". NASA CR-167952, (1982).

[8] S. Lewy. "Prediction of turbofan rotor or stator broadband noise radiation". *Acta Acustica*, 93 (2):275–283, (2007).

[9] S.W. Rienstra. "Acoustic radiation from a semi-infinite annular duct in a uniform subsonic mean flow". *Journal of Sound and Vibration*, 94 (2):267–288, (1984).